



Simulation of Stochastic Wind Field on Long Span Cable-stayed Bridge

Yongyi Yang¹, Zizhen Zhang^{2,*}, Jizhong Yang³

¹XIHUA University, Chengdu, Sichuan 610031, China

²Kunming Atide Software Co., Ltd, Kunming, Yunnan, 650106, China

³China railway eryuan engineering group Co. LTD, Chengdu, 610031, China

*Corresponding author. zhangzz@atidesoft.com

Abstract. The quick and efficient simulation of wind speed profiles is a necessary condition for performing time history response analysis of bridges. This paper introduces the harmonic synthesis method for simulating wind fields and applies it to simulate the random wind field at the location of the Hanjia River Yangtze River Bridge on the Yuli Railway. The paper also provides a detailed comparison of the effects of different aerodynamic admittance functions on the fluctuating wind speed spectrum. The explicit Cholesky decomposition of the wind speed spectrum density matrix is performed, and the simulation efficiency is greatly improved by using FFT techniques. A wind field simulation program is developed, and the correctness of the program is verified by comparing the wind speed spectrum and correlation functions, laying a solid foundation for the effective analysis of wind-induced vibrations in structures.

Keywords: cable-stayed, FFT, Bridge, Stochastic wind field.

1 Introduction

To perform time history analysis of large-span bridge structures under buffeting vibrations, it is necessary to first computationally simulate a random wind field. The Monte Carlo method is a direct and effective approach that utilizes computational simulation techniques to generate random wind speed samples for atmospheric boundary layer wind fields with given spectral characteristics. These samples are then used to analyze the dynamic response of the structure using linear or nonlinear methods.

From prior studies, natural wind turbulence may be modeled as a consistent Gaussian random process. If we view the wind's pattern as an accumulation of random wind waves across specific spatial positions, we can analyze the random pattern as a one-dimensional multivariate random process. When employing the Monte Carlo method, there exist two primary approaches for simulating such multivariate random processes.

The first category is the harmonic synthesis method (WAWA method). Harmonic synthesis is a traditional method that utilizes spectral decomposition and trigonometric series superposition to simulate samples of random processes. Rice^[1] proposed the basic idea of harmonic synthesis, initially only able to simulate one-dimensional,

© The Author(s) 2024

P. Xiang et al. (eds.), *Proceedings of the 2023 5th International Conference on Hydraulic, Civil and Construction Engineering (HCCE 2023)*, Atlantis Highlights in Engineering 26,

https://doi.org/10.2991/978-94-6463-398-6_66

single-variable stationary Gaussian random processes. Borgman [2] and Shinozuka [3] addressed the simulation problem of multi-dimensional, multivariate, and even non-stationary random processes. Their methods have been widely applied and continuously improved. Yang [4] integrated FFT techniques into the computations, greatly improving the computational efficiency of this type of method. Yamazaki [5] proposed the iterative WAWS method for simulating non-stationary random processes, and Deodatis [6] introduced the concept of frequency bivariate indexing and proposed a new harmonic synthesis method for simulating multivariate stationary Gaussian random processes. Cao Yinghong applied the explicit decomposition of the spectral matrix in special cases, significantly improving the computational efficiency of this method, and successfully simulated the fluctuating wind speed of the main beam of a large-span bridge.

The second category of methods utilizes linear filtering techniques (such as AR, MA, ARMA, etc.). Linear filtering techniques are widely used in the analysis of random vibrations and time series analysis. Gerch [7] was one of the early researchers who applied linear filtering techniques to generate random time series and other engineering problems. This method opened up a new approach for random simulation due to its convenience and speed. Since then, many scholars have continuously improved the linear filtering method, developing it to simulate multi-dimensional and multivariate random processes using AR, MA, and ARMA models. Spanos, Samaras, Mignolet, Li & Kareem, Paola, and other researchers have made significant contributions in this field [8-12]. Reed & Scanlan, Iazzunni, Huang, and others have applied these methods in the simulation of turbulent wind fields [13-15]. Among them, the autoregressive model AR(p) for multivariate random processes is widely used in the linear filtering method.

This paper focuses on the engineering context of the Hanjia River Yangtze River Bridge, specifically the 432m main span of the Yuli Railway. It utilizes the harmonic synthesis method (WAWS method) to replicate the random wind conditions around the bridge. The simulation takes into account various aerodynamic admittance functions, verifying the accuracy of the simulated random wind by comparing power spectra and correlation functions.

2 Fluctuating Wind Speed Spectrum

In the process of wind field simulation, due to the lack of observed data for strong wind fluctuation time history at the bridge site, the wind spectra and coherence functions in the bridge site area are expressed using commonly used forms from foreign sources. The spectra for the transverse and longitudinal wind speeds are represented by Simiu spectra that vary with height, while the vertical wind speed spectrum is represented by the Lumley-Panofsky spectrum.

Simiu Transverse and Longitudinal Wind Speed Spectra:

$$\frac{nS_u(f)}{u_*^2} = \frac{200f}{(1+50f)^{5/3}}, \quad \frac{nS_v(f)}{u_*^2} = \frac{15f}{(1+9.5f)^{5/3}} \quad (1)$$

Lumley-Panofsky Vertical Wind Speed Spectrum:

$$\frac{nS_w(f)}{u_*^2} = \frac{3.36f}{(1+10f)^{5/3}} \tag{2}$$

Where: f - Monin-Obukhov coordinate; n - Frequency; u^* - Friction velocity. The coherence function is expressed using the Davenport form:

$$Coh_{jm}(\omega) = \exp\left(-\lambda \frac{\omega r_{jm}}{2\pi U_z}\right) \tag{3}$$

Where: λ - Dimensionless attenuation factor, conservatively taken as 7; U_z — Mean wind speed at height Z ; r_{ij} — - Distance between points j and m .

3 Pneumatic admittance function

The approach adopted in this paper involves employing the harmonic synthesis technique for simulating the fluctuating wind patterns. In the case of a zero-mean, one-dimensional Gaussian process with n variables, the cross-spectral density matrix is expressed by the equation.

$$S^0(\omega) = \begin{bmatrix} S_{11}^0(\omega) & S_{12}^0(\omega) & \cdots & S_{1n}^0(\omega) \\ S_{21}^0(\omega) & S_{22}^0(\omega) & \cdots & S_{2n}^0(\omega) \\ \cdots & \cdots & \cdots & \cdots \\ S_{n1}^0(\omega) & S_{n2}^0(\omega) & \cdots & S_{nn}^0(\omega) \end{bmatrix} \tag{4}$$

The Cholesky decomposition is applied to matrix $S^0(\omega)$ in equation:

$$S^0(\omega) = H(\omega)H^{T*}(\omega) \tag{5}$$

where $H(\omega)$ is the lower triangular matrix and $H^{T*}(\omega)$ is its complex conjugate transpose.

$$H(\omega) = \begin{bmatrix} H_{11}(\omega) & 0 & \cdots & 0 \\ H_{21}(\omega) & H_{22}(\omega) & \cdots & 0 \\ \cdots & \cdots & \cdots & \cdots \\ H_{n1}(\omega) & H_{n2}(\omega) & \cdots & H_{nn}(\omega) \end{bmatrix} \tag{6}$$

In equation (6), the diagonal elements are non-negative real functions of ω , and the off-diagonal elements are generally complex functions of ω .

For the diagonal elements

$$H_{jj}(\omega) = H_{jj}(-\omega) \quad j = 1, 2, \dots, n$$

For the off-diagonal elements

$$H_{jm}(\omega) = |H_{jm}^*(-\omega)| e^{i\theta_{jm}(\omega)}$$

Where:

$$j = 1, 2, \dots, n, \quad m = 1, 2, \dots, j-1;$$

$$\theta_{jm}(\omega) = \tan^{-1} \left\{ \frac{\text{Im}[H_{jm}(\omega)]}{\text{Re}[H_{jm}(\omega)]} \right\}$$

As $N \rightarrow \infty$, the samples of the random process can be simulated using the following equation^[16]:

$$f_j(t) = 2\sqrt{\Delta\omega} \sum_{m=1}^j \sum_{l=1}^N |H_{jm}(\omega_{ml})| \cos(\omega_{ml}t - \theta_{jm}(\omega_{ml}) + \phi_{ml}) \quad (7)$$

Where $j = 1, 2, \dots, n$; N is the frequency subdivision number;

$\Delta\omega$ is the frequency increment, $\Delta\omega = \frac{\omega_u}{N}$;

ω_{ml} is the double-index frequency, $\omega_{ml} = l\Delta\omega - \frac{N-m}{N}\Delta\omega = (l-1)\Delta\omega + \frac{m}{N}\Delta\omega$;

ϕ_{ml} is an independently random phase uniformly distributed between 0 and 2π ;

ω_u is the upper cutoff frequency, which can be estimated using the following equation,

$$\int_0^{\omega_u} S(\omega) d\omega = (1 - \varepsilon) \int_0^{\infty} S(\omega) d\omega$$

Where $S(\omega)$ is the power spectral density function, and ε is much smaller than 1 (such as 0.01 or 0.001).

By applying FFT techniques, the formula for simulating the wind speed time history can be written as follows:

$$f_j(p\Delta t) = \text{Re} \left\{ \sum_{m=1}^j h_{jm}(q\Delta t) \exp \left[i \left(\frac{m\Delta\omega}{n} \right) (p\Delta t) \right] \right\} \quad (8)$$

Where $p=0, 1, 2, \dots, M \times n - 1$; $q=0, 1, 2, \dots, 2N - 1$; $M \geq 2N$;

$$h_{jm}(q\Delta t) = \sum_{l=0}^{2N-1} B_{jm}(l\Delta\omega) \exp[i(l\Delta\omega)(q\Delta t)] \quad (9)$$

The value of $B_{jm}(l\Delta\omega)$ can be determined using the following equation:

$$B_{jm}(l\Delta\omega) = \begin{cases} \sqrt{2(\Delta\omega)}H_{jm}(l\Delta\omega + \frac{m\Delta\omega}{n})\exp(i\phi_{ml}) & 0 \leq l \leq N \\ 0 & N \leq l \leq M-1 \end{cases} \tag{10}$$

From equation (10), $h_{jm}(q\Delta t)$ can be seen that can be computed efficiently using FFT techniques, significantly reducing computational workload.

In long-span cable-stayed and suspension bridges, the main girder typically maintains a consistent height throughout its entirety. Under minimal variation in topography across the transverse direction, an assumption can be made that simulated points along the main girder share an equivalent mean wind speed and pulsating wind speed spectrum, thereby.

$$S_{11}^0(\omega) = S_{22}^0(\omega) = \dots = S_{mm}^0 = S(\omega) \tag{11}$$

In this case,

$$S_{jm}^0(\omega) = \sqrt{S_{jj}^0(\omega)S_{mm}^0(\omega)}\text{Coh}_{jm}(\omega) = S(\omega)\text{Coh}_{jm}(\omega) \tag{12}$$

When the simulated points are equidistantly arranged, $r_{jm} = \Delta|j-m|$, with a spacing of Δ , the coherence function can be written as:

$$\text{Coh}_{jm}(\omega) = \left(\exp\left(-\lambda \frac{\omega\Delta}{2\pi U_z}\right) \right)^{|j-m|} = (\cos\alpha)^{|j-m|} \tag{13}$$

where: $\cos\alpha = \exp\left(-\lambda_{ij} \frac{\omega\Delta}{2\pi V_z}\right)$.

The cross-spectrum can be written in the following form:

$$S^0(\omega) = S(\omega) \begin{bmatrix} 1 & & & & \text{Symm} \\ \cos\alpha & 1 & & & \\ (\cos\alpha)^2 & \cos\alpha & 1 & & \\ \vdots & \vdots & \vdots & \ddots & \\ (\cos\alpha)^{n-1} & (\cos\alpha)^{n-2} & (\cos\alpha)^{n-3} & \dots & 1 \end{bmatrix} \tag{14}$$

By using an analytical method, an explicit expression for the Cholesky decomposition $H(\omega)$ of the above equation can be obtained, as shown in equation (16), where.

$$H(\omega) = \sqrt{S(\omega)}G(\omega) \tag{15}$$

where:

$$G(\omega) = \begin{bmatrix} 1 & & & & 0 \\ \cos \alpha & \sin \alpha & & & \\ (\cos \alpha)^2 & \sin \alpha \cos \alpha & \sin \alpha & & \\ \vdots & \vdots & \vdots & \ddots & \\ (\cos \alpha)^{n-1} & \sin \alpha (\cos \alpha)^{n-2} & \sin \alpha (\cos \alpha)^{n-3} & \cdots & \sin \alpha \end{bmatrix} \quad (16)$$

The above equation can be written in algebraic form as:

$$G_{jm}(\omega) = \begin{cases} 0 & 1 \leq j < m \leq n \\ (\cos \alpha)^{|j-m|} & m = 1, m \leq j \leq n \\ \sin \alpha (\cos \alpha)^{|j-m|} & 2 \leq m \leq j \leq n \end{cases} \quad (17)$$

4 Simulation of Random Wind Field^[17]

A simulation of the random wind field at the main beam of the Hanjiatu Yangtze River Bridge was conducted using the harmonic synthesis method. The equivalent spectral method was employed to simulate the wind field. The influence of aerodynamic admittance functions was taken into account. Three types of aerodynamic admittance functions were considered:

(1) No consideration of the aerodynamic admittance function, i.e., setting the aerodynamic admittance function equal to 1.

(2) Adoption of the Sears aerodynamic admittance function for lift and moment admittances:

$$|\chi(k)|^2 = \frac{1}{1 + \pi k}, \quad k = \frac{\omega B}{U} \quad (18)$$

(3) Adoption of the aerodynamic admittance functions derived from the study of the Balinhe River Extra-large Bridge:

Lift admittance function:

$$|\chi_L(k)|^2 = \frac{1.331}{1 + 1.737k^{0.616}} \quad (19)$$

Drag admittance function:

$$|\chi_D(k)|^2 = \frac{1.286}{1 + 2.99k^{0.574}} \quad (20)$$

Moment admittance function:

$$|\chi_M(k)|^2 = \frac{0.394}{1 + 0.003k^{3.413}} \tag{21}$$

where k is the reduced frequency, B is the bridge width, and U is the mean wind speed.

Table 1 displays the simulation and calculation parameters. Figures 1 and 2 show-case the simulation results, whereas Figure 3 offers a juxtaposition of the target spectrum and simulated spectrum, along with the target correlation function and simulated correlation function. The visuals illustrate a compelling alignment between the power spectral density curves and correlation function curves in comparison to the target curves, affirming a commendable simulation performance.

Table 1. Parameters for Simulating Turbulent Wind Speed

Bridge Span	864m	Cutoff Frequency	4π
Height of Main Beam from Ground	69m	Fraction of Frequencies	2048
Surface Roughness	0.22m	Sampling Time Interval	0.04s
Average Wind Speed at the Main Beam	29.0	Number of Simulated Samples	8192
Number of Simulation Points	65	Horizontal Wind Spectrum	Simiu spectrum
Spacing between Simulation Points	13.5m	Vertical Wind Spectrum	Lumley-Panofsky spectrum

Due to the lack of observed data on strong wind fluctuation time history at the bridge site, the wind spectrum and coherence function at the bridge site are expressed using commonly used forms from international sources. The lateral and longitudinal wind speed spectra adopt the Simiu spectrum, which varies with height, while the vertical wind speed spectrum adopts the Lumley-Panofsky spectrum.

Simiu Spectrum for Lateral and Longitudinal Wind Speeds:

$$\frac{nS_u(f)}{u_*^2} = \frac{200f}{(1 + 50f)^{5/3}}, \quad \frac{nS_v(f)}{u_*^2} = \frac{15f}{(1 + 9.5f)^{5/3}} \tag{22}$$

Lumley-Panofsky Spectrum for Vertical Wind Speed:

$$\frac{nS_w(f)}{u_*^2} = \frac{3.36f}{(1 + 10f)^{5/3}} \tag{23}$$

Where: f - Monin-Obukhov coordinate, n - frequency, u^* - friction velocity. The coherence function is formulated using the Davenport expression:

$$Coh_{jm}(\omega) = \exp\left(-\lambda \frac{\omega r_{jm}}{2\pi U_Z}\right) \tag{24}$$

Where: λ - dimensionless attenuation factor, conservatively taken as 7; U_Z - mean wind speed at height Z ; r_{jm} - distance between points j and m .

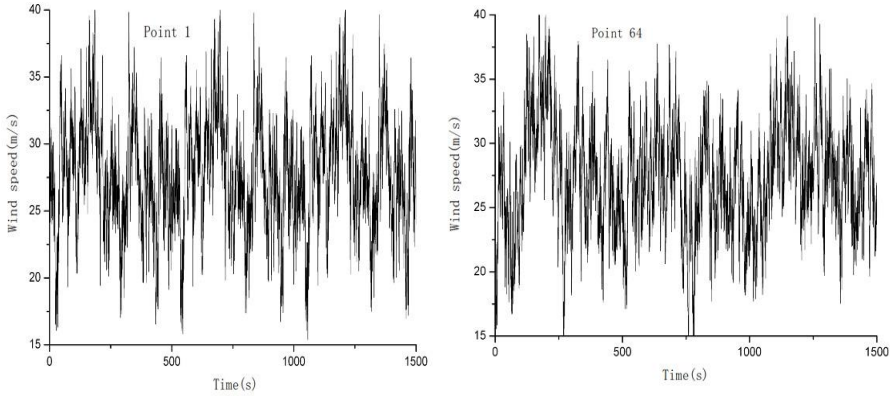


Fig. 1. Partial Time History of Horizontal Wind Speed at Points 1 and 64

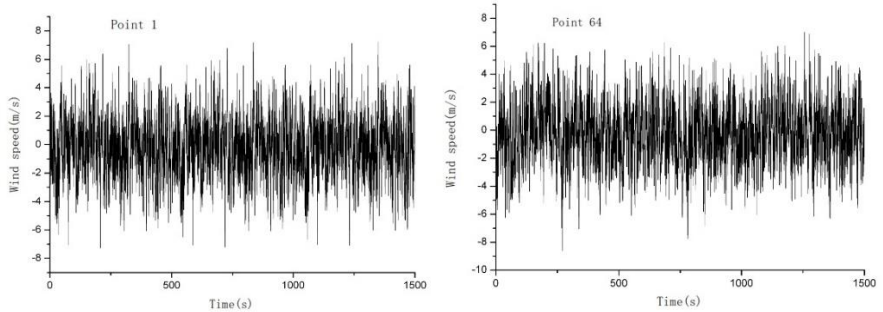
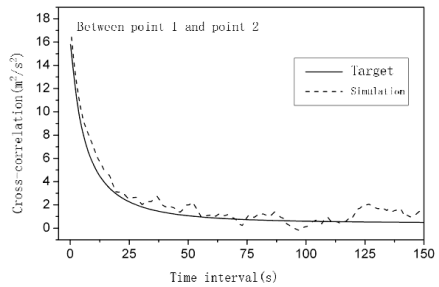
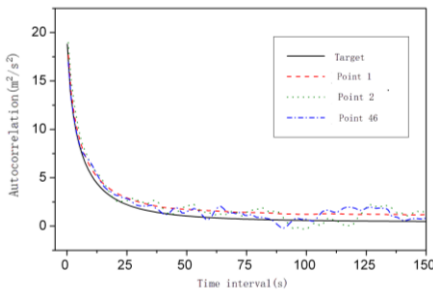


Fig. 2. Partial Time History of Vertical Wind Speed at Points 1 and 64



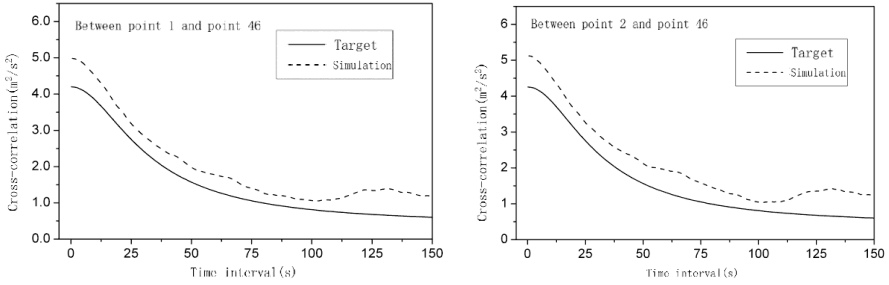


Fig. 3. represents the correlation function of the pulsating wind field in the transverse direction of the main beam

5 Conclusions

Accurate simulation of wind speed timelines is crucial for analyzing bridge responses in the time domain. This paper presents the harmonic synthesis method to simulate wind fields. It derives the explicit expression for Cholesky decomposition of the cross-spectral density matrix and enhances simulation efficiency using FFT techniques. Furthermore, the paper extensively compares how various aerodynamic admittance functions impact the pulsating wind speed spectrum. It concludes by developing a wind field simulation program and showcasing a case study of the Hanjiatuo Yangtze River Bridge on the Yuli Railway. This work forms a strong basis for effective structural time-domain analysis of wind-induced vibrations.

Acknowledgment

Sichuan Provincial Natural Science Foundation, (No.:2023NSFC0389).

Yunnan Provincial Science and Technology Plan Project, (No.: 202305AF150138).

Yunnan Prov. Sci. & Tech. Spec. Plan, (NO.: 202102AD080003).

Sichuan Sci. & Tech. Program (No:2021YFG0065).

References

1. Rice S O. Mathematic analysis of random noise. Selected papers on noise and stochastic processes, N. Wax, editor, Dover publish Incorporated, New York, N.Y., 1954:133-294.
2. Borgman L E. Ocean wave simulation for engineering design. *Journal of Waterway, Port, Coastal, and Ocean Engineering ASCE*, 1969, 95(4):557-583.
3. Shinozuka M, et al. Digital simulation of random processes and its application. *Journal Sound and Vibration*, 1972, 25(1):111-128.
4. Yang J N. Simulation of random envelope processes. *Journal Sound and Vibration*.1972, 25(1):73-85.
5. Yamazaki F, et al. Digital generation of non-Gaussian stochastic fields. *Journal of Engineering Mechanics ASCE*, 1988, 114(7):1183-1197.

6. Deodatic G. Simulation of ergodic multivariate stochastic processes. *Journal of Engineering Mechanics ASCE*, 1996, 122(8):778-787.
7. Gerch W, et al. Synthesis of multi-variate random vibration systems: a two stage least squares ARMA model approach. *Journal Sound and vibration*, 1977, 52(4):553-565.
8. Spanos P D, et al. Monte Carlo treatment of random fields: a broad perspective. *Applied Mechanics Reviews* 1988, 51(3):219-237.
9. Samaras E, et al. ARMA representation of random processes. *Journal of Engineering Mechanics ASCE*, 1985, 111(3):449-461.
10. Mignolet M P, et al. MA to ARMA modeling of wind. *Journal of Wind Engineering and Industrial Aerodynamic* 1990, 36:429-438.
11. Li Y, et al. Simulation of multivariate random processes: hybrid DFT and digital filtering approach. *Journal of Engineering Mechanics* 1993, 119(3):1078-1098.
12. Paola M D. Digital simulation of wind field velocity. *Journal of Wind Engineering and Industrial Aerodynamic* 1998, 74-76:91-109.
13. Reed D A, et al. Time series analysis of cooling tower wind loading. *Journal of Structural Engineering Division ASCE*, 1987, 109(2):538-554.
14. Iazzunni A, et al. Artificial wind generation and structural response. *Journal of Structural Engineering Division ASCE*, 1987, 113(12)2383-2397.
15. Huang Z, et al. Use of time –series analysis to model and forecast wind speed. *Journal of Wind Engineering And Industrial Aerodynamics*.1995, 56:311-322.
16. Shinozuka M. et al. Simulation of stochastic processes by spectral representation. *Applied Mechanics Reviews* 1991, 44(4):191-204.
17. YANG Yong-yi. *Wind Tunnel Tests for Long Span Railway Cable-Stayed Bridge[D]*. Southwest Jiaotong University,2011.

Open Access This chapter is licensed under the terms of the Creative Commons Attribution-NonCommercial 4.0 International License (<http://creativecommons.org/licenses/by-nc/4.0/>), which permits any noncommercial use, sharing, adaptation, distribution and reproduction in any medium or format, as long as you give appropriate credit to the original author(s) and the source, provide a link to the Creative Commons license and indicate if changes were made.

The images or other third party material in this chapter are included in the chapter's Creative Commons license, unless indicated otherwise in a credit line to the material. If material is not included in the chapter's Creative Commons license and your intended use is not permitted by statutory regulation or exceeds the permitted use, you will need to obtain permission directly from the copyright holder.

